Raman scattering, spectropolarimetry and symbiotic stars

H. Schild and H. M. Schmid

The spectra of symbiotic stars simultaneously exhibit the signature of a cool giant and an ionised nebulosity. Symbiotic stars are unresolved binary systems consisting of a mass-losing red giant and a hot radiation source with an effective temperature of typically around ~100,000 K. The nebulosity is thought to be the ionised stellar wind of the red giant. The orbital periods of these binaries range from several hundred days to a few decades. At present, the count of known symbiotic stars has reached 150, most of which are galactic stars. A handful have however been detected in the Magellanic Clouds and in another nearby local group galaxy.

The spectra of symbiotic stars often show two emission lines at λ6825 and λ7082, which are much broader than the other emission lines in the spectrum (see Figure 1). Up to now these two emissions have only been observed in symbiotic systems with high excitation nebulae. After many years of fruitless search for a plausible identification for these lines, the puzzle seems finally to have been solved: the $\lambda\lambda$6825, 7082 lines are probably due to Raman scattering of the OVI $\lambda\lambda$1032, 1038 resonance lines by neutral hydrogen as was recently pointed out by H. M. Schmid. Unlike Rayleigh scattering where the emitted photon has the same energy as the incoming photon, Raman scattering is non-elastic. Figure 2 shows schematically the process in question: an incoming OVI photon with frequency υ_i could in energy terms excite hydrogen from its ground state 1*s* ^{2}S to a virtual state *m*. After the scattering process hydrogen is left in the 2*s* ^{2}S state while the surplus energy was radiated away with frequency υ_f by the Raman-scattered photons. Energy conservation requires that the frequencies of the incident and the scattered photon are related by

$$\upsilon_f = \upsilon_i - \upsilon_{if}.$$

υ_{if} is the frequency corresponding to the energy difference between the initial *i* and final *f* atomic states. If the incident radiation is OVI $\lambda\lambda$1032,38 the outcoming photons have the wavelength required to match the features observed in symbiotic stars. The OVI photons as seen by the H° scatterers will normally have a small frequency displacement $\upsilon_i' = \upsilon_i + \Delta\upsilon$, for example due to Doppler broadening. The frequency of the scattered photon will then be displaced by the same amount according to $\upsilon_f' = \upsilon_f + \Delta\upsilon$. This means for the relative line width, that

$$\frac{\Delta\upsilon}{\upsilon_f} = \frac{\upsilon_i}{\upsilon_f}\frac{\Delta\upsilon}{\upsilon_i}$$

or the relative line widths for Raman scattered OVI lines are approximately 7 times broader than the original OVI emission line. This explains the large line widths observed in the $\lambda\lambda$6825, 7082 features.

Raman scattering is a well-known physical process and it is widely used in the laboratory to study molecular spectra. The mechanism is exploited commercially in tunable lasers. Raman and Rayleigh scattering are closely associated processes and commonly occur in planetary atmospheres. The red emission features in symbiotic spectra however are the first manifestation of Raman

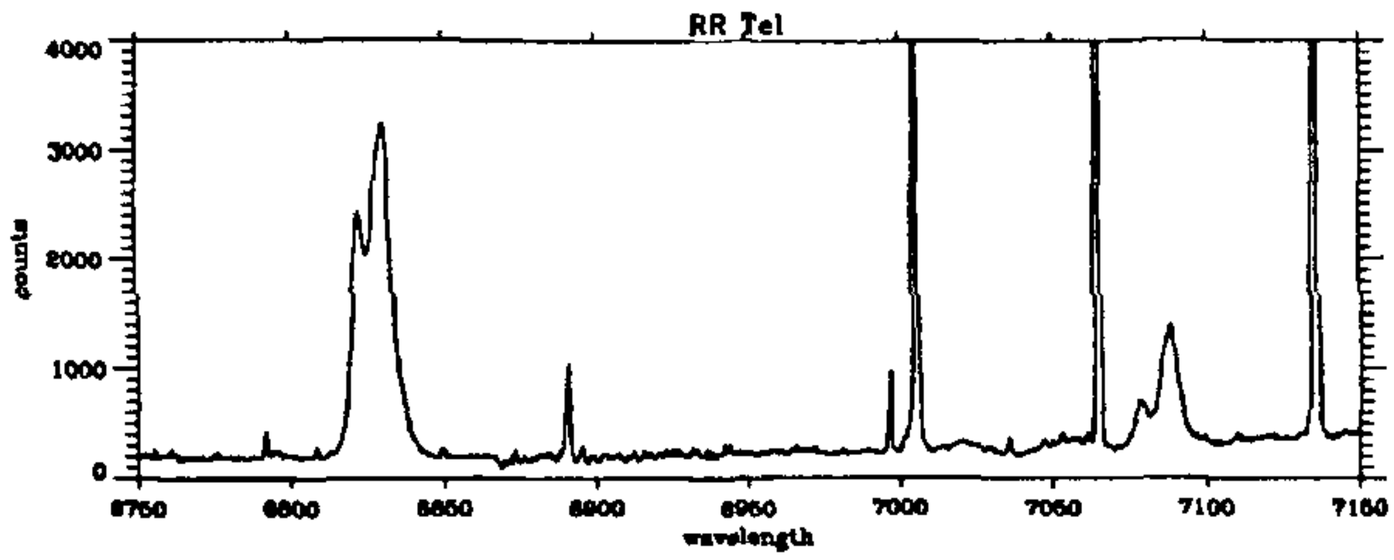

Figure 1. Red spectrum of RR Tel showing the two broad Raman features at λ6825 and λ7082. Note that in this particular symbiotic system the features are double-peaked. The narrow lines are collisionally excited or recombination nebular lines (courtesy of H. Duerbeck and H. Schwarz).

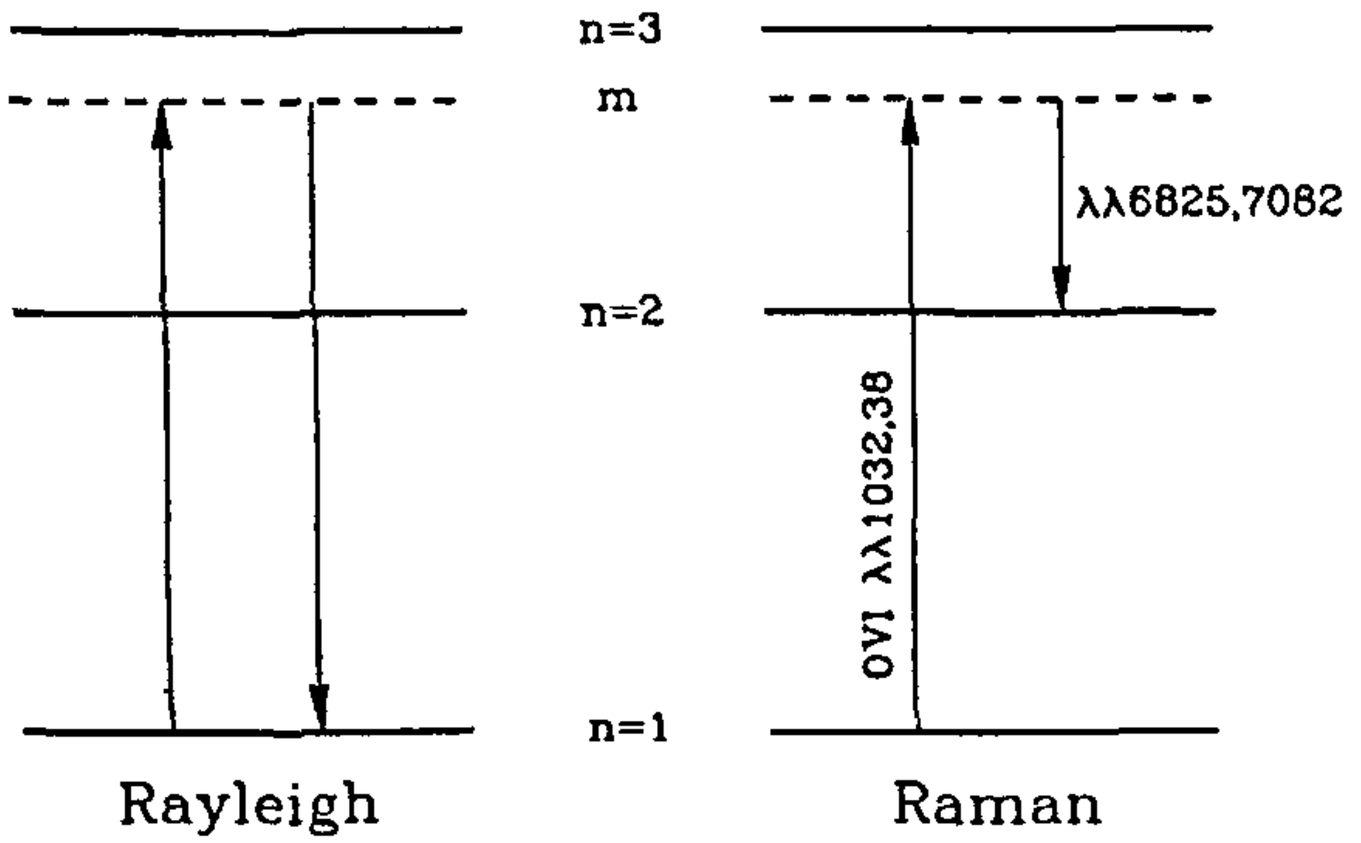

Figure 2. Schematic energy level diagram of hydrogen showing the processes of Rayleigh and Raman scattering. The wavelengths of the incident and scattered photons as observed in symbiotic stars are shown as an illustration.

Reprinted with permission from *Gemini*, No. 37, September 1992.

scattering of emission lines in an astronomical object.

The cross section for Raman scattering of OVI photons by neutral hydrogen is very small and special conditions, for the process to be observable, are required. In symbiotic systems all the ingredients are available in sufficient amounts. The strong OVI lines are produced in the innermost part of the nebulosity near the hot component (see Figure 3). Although the OVI lines are not directly observable with present-day UV satellite observatories, there is ample indirect evidence for their existence from other strong emission lines from highly ionised species like FeVII, MgV or NeV. The OVI photons get converted near the neutral surface of the cool giant into the $\lambda\lambda$6825, 7082 photons. In no other astrophysical object is high-density neutral hydrogen so strongly irradiated by OVI photons and it is, after all, not so surprising that these emission lines have only been observed in symbiotic systems.

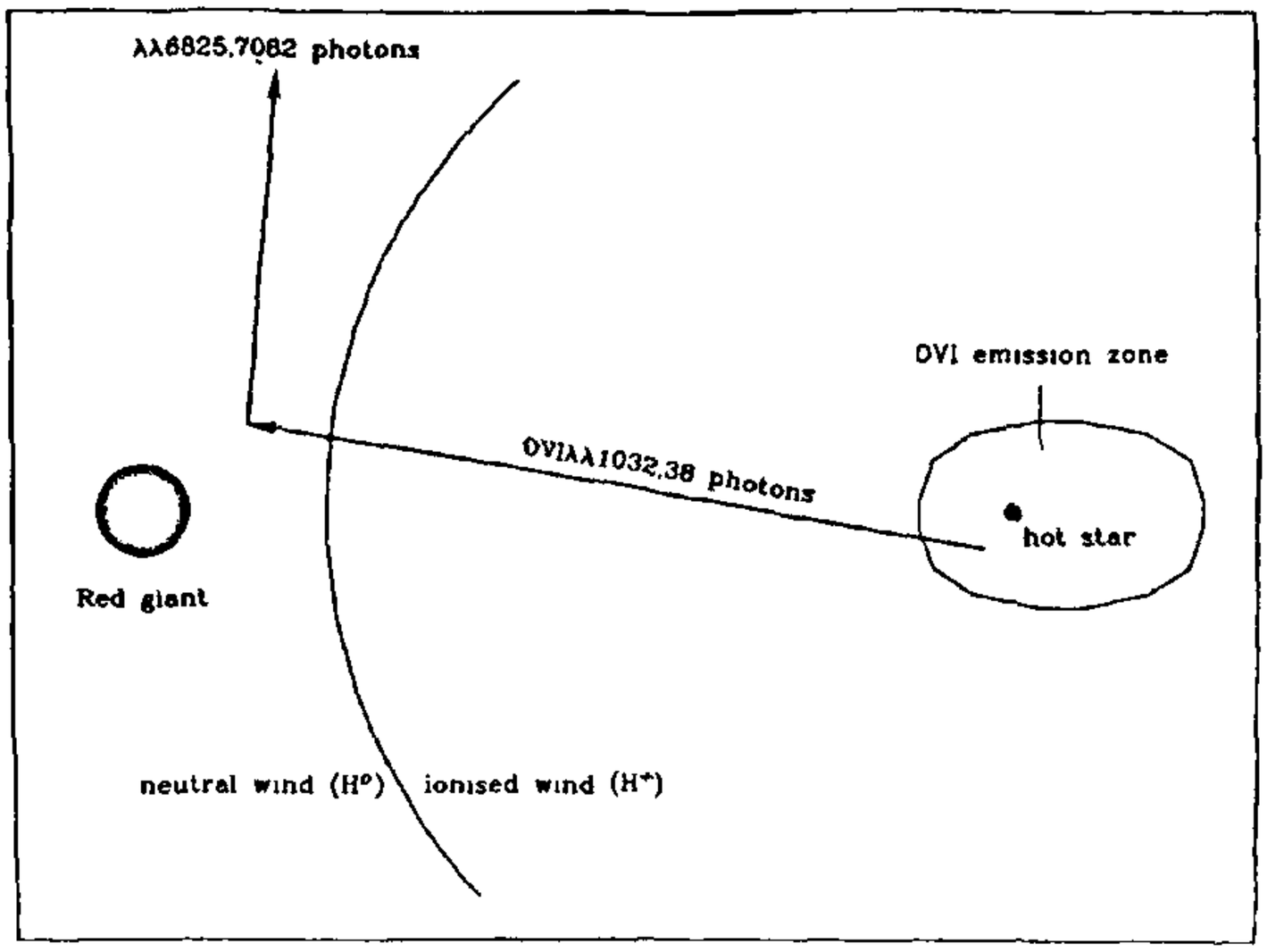

Figure 3. Sketch of a symbiotic binary system. The hot companion source (on the right) ionizes part of the stellar wind of a red giant (left). The OVI $\lambda\lambda$1032,38 photons are generated near the hot source. The Raman scattering zone is close to the red giant.

WHT spectropolarimetry

Raman (like Rayleigh) scattering is a dipole type scattering process which produces light polarization. Only a very small net polarization would however be observed if scattering took place in a (circumstellar) nebula, because rotational symmetry with respect to the line of sight tends to compensate the polarization from different scattering regions. There is however a pronounced anisotropy in the scattering geometry in symbiotic systems, as photons are produced by or near the hot component and scattered near the red giant star. Another polarization-enhancing factor is that all photons in the Raman lines $\lambda\lambda$6825, 7082 are produced by a scattering process. In contrast to coherent scattering (like Rayleigh and Thomson scattering) the polarization in the Raman scattered lines is not diluted by light coming directly i.e. unscattered from the source. All these factors combine in the expectation that the $\lambda\lambda$6825, 7082 emission lines are highly polarized ($\sim$10%).

First exploratory spectropolarimetric observations by Schild during an observing run, which not surprisingly had been approved for a completely different programme, showed mixed results. In the symbiotic star He2-38 a polarization of 5.3 and 9.2% was observed in the 6825 and 7082 Å features respectively but no polarization was found in the other object RX Pup. We were subsequently allocated a WHT service night during which six symbiotic stars were observed by Clive Tadhunter with ISIS and the spectropolarimeter (R600R grating). Each object was observed with the half-wave plate at four different angles. Typical exposure times were 600 s at each angle of the half-wave plate. Polarization was found to be clearly present in the λ6825 line in all six objects. This therefore constitutes

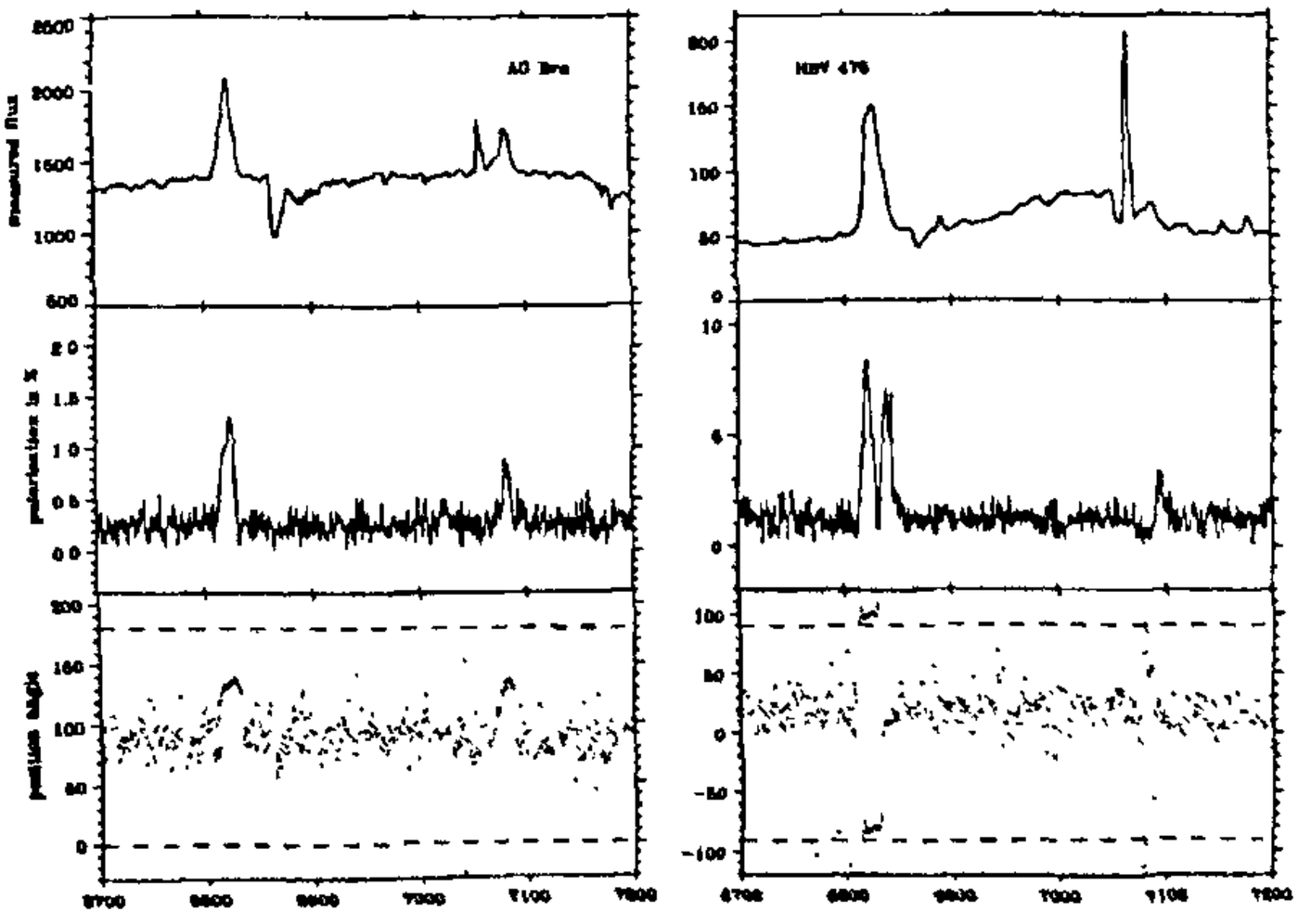

Figure 4 a. WHT spectropolarimetric observations of AG Dra and HBV 475. The three panels show from top to bottom rectified total flux, percentage polarization and position angle of the polarization vector. The narrow emission line is HeI λ7065

additional observational evidence that Raman scattering is indeed responsible for the formation of the $\lambda\lambda$6825,7082 emission lines. Figure 4*a* shows the WHT observations of AG Dra and HBV 475. Evidently, there is additional polarization in the λ6825 and the λ7082 features above the polarization of the continuum and the HeI λ7065 recombination line which is due to interstellar grains.

Besides this, and very interestingly, the WHT observations revealed that there were structural variations in the degree and angle of the polarization across the line profile. In HBV 475 the polarization across the λ6825 line is double-peaked and the blue and red wings have polarization angles $-80°$ and $+10$ respectively, being thus perpendicularly polarized (Figure 4*b*). The same polarization pattern is also present in the λ7082 line. HBV 475 was in orbital phase 0.74 at the time of the

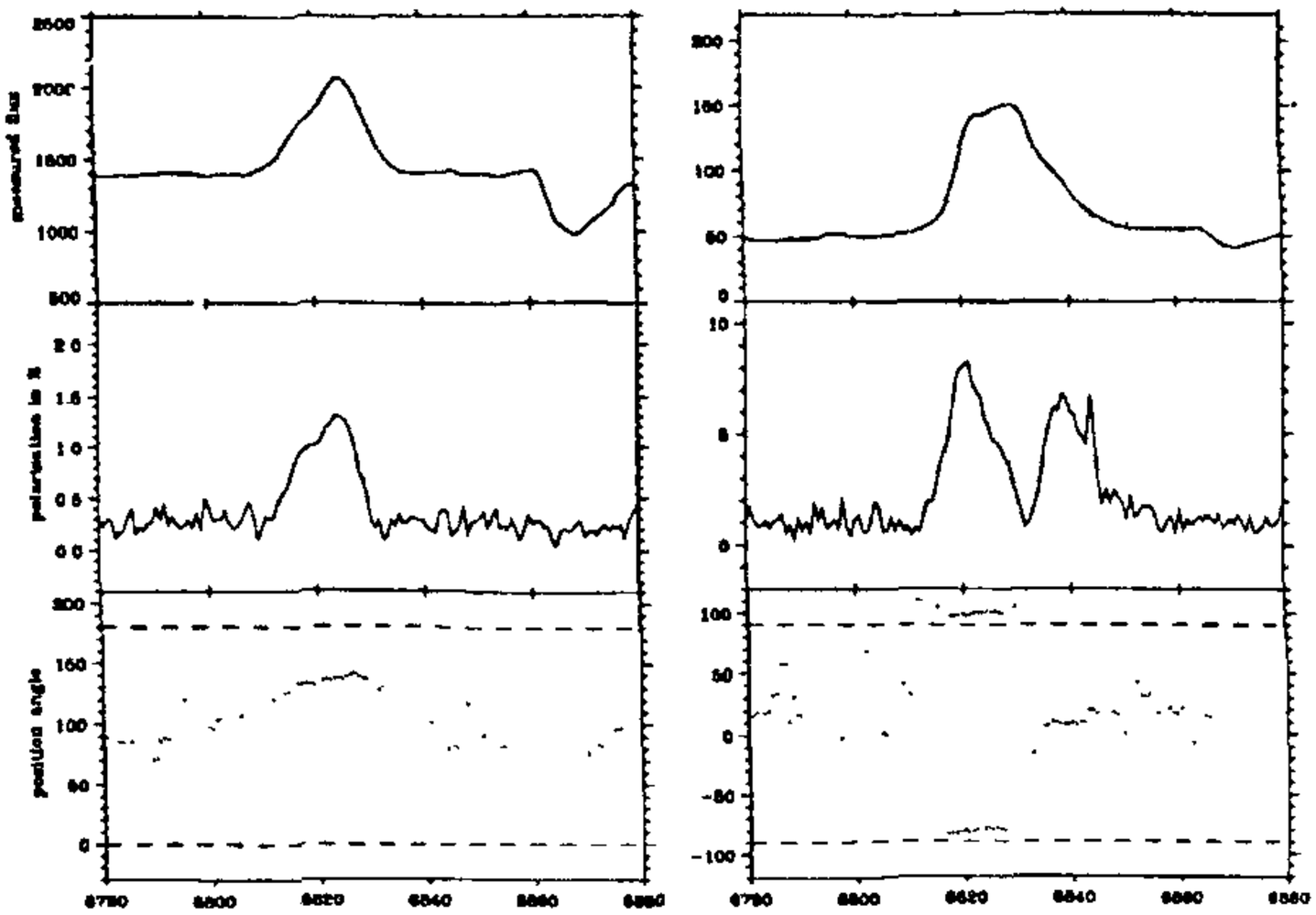

Figure 4 b. Enlargement of Figure 4 a showing only the λ6825 feature of AG Dra (left) and HBV 475 Note the double-peaked polarization profile and the flip of 90° in the polarization angle in HBV 475

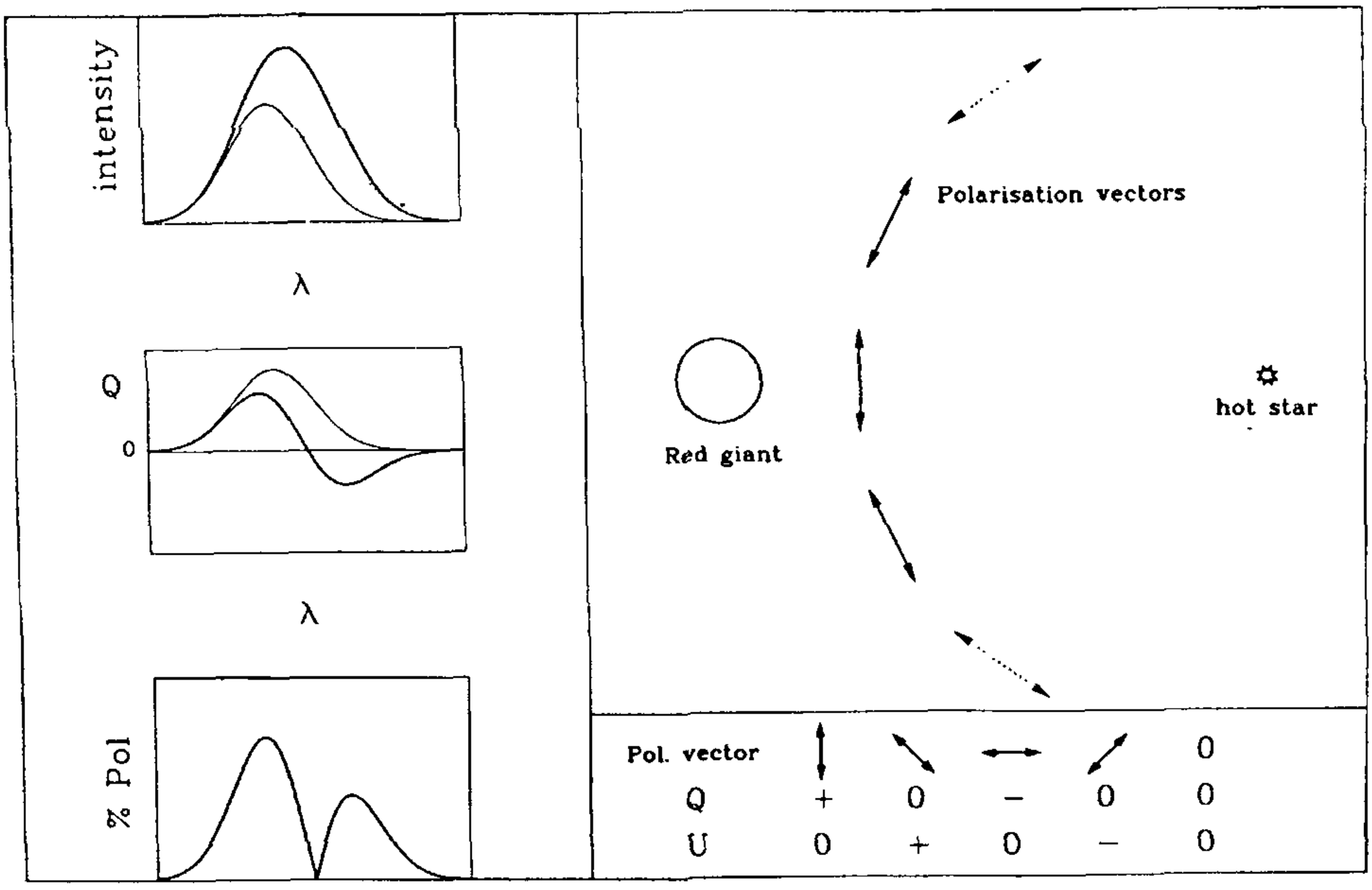

Figure 5. Illustration of the polarization structure in HBV 475 Upper right panel The polarization vectors of the Raman scattered light shown for the same symbiotic configuration as in Figure 3 Lower right panel *Q* and *U* Stokes parameter an observer would measure for a given orientation of the polarization vectors Left panel The resulting total intensity. Stokes *Q* and percentage polarization across a Raman scattered emission line as observed from the (usually) spatially unresolved symbiotic system The polarization vectors plotted in dotted and continuous lines produce the respective contributions in the graphs. The summed quantities are plotted as thick lines Note the resulting double-peaked polarization profile (lower left)

observation For a simplified interpretation of this polarization structure consider Figure 5. Blue and red shifted scattered photons are produced according to the relative motion of the particles in the neutral wind of the red giant with respect to the OVI source. Scattering near the binary axis produces the blue and vertically polarized wing of the λ6825 profile as indicated by the continuous polarization vectors. The polarization vectors which contribute to the red and horizontally polarized wing are plotted in dotted lines. The respective contributions to the intensity, Stokes Q parameter and percentage polarization are shown schematically in the same line styles in the graphs on the left. Because of the axial symmetry of the configuration, the Stokes U components cancel and

$$P=\frac{\sqrt{Q^2+U^2}}{I}=\frac{|Q|}{I}.$$

Thus only vertically or horizontally polarized radiation emerges, which explains the 90° flip of the polarization angle.

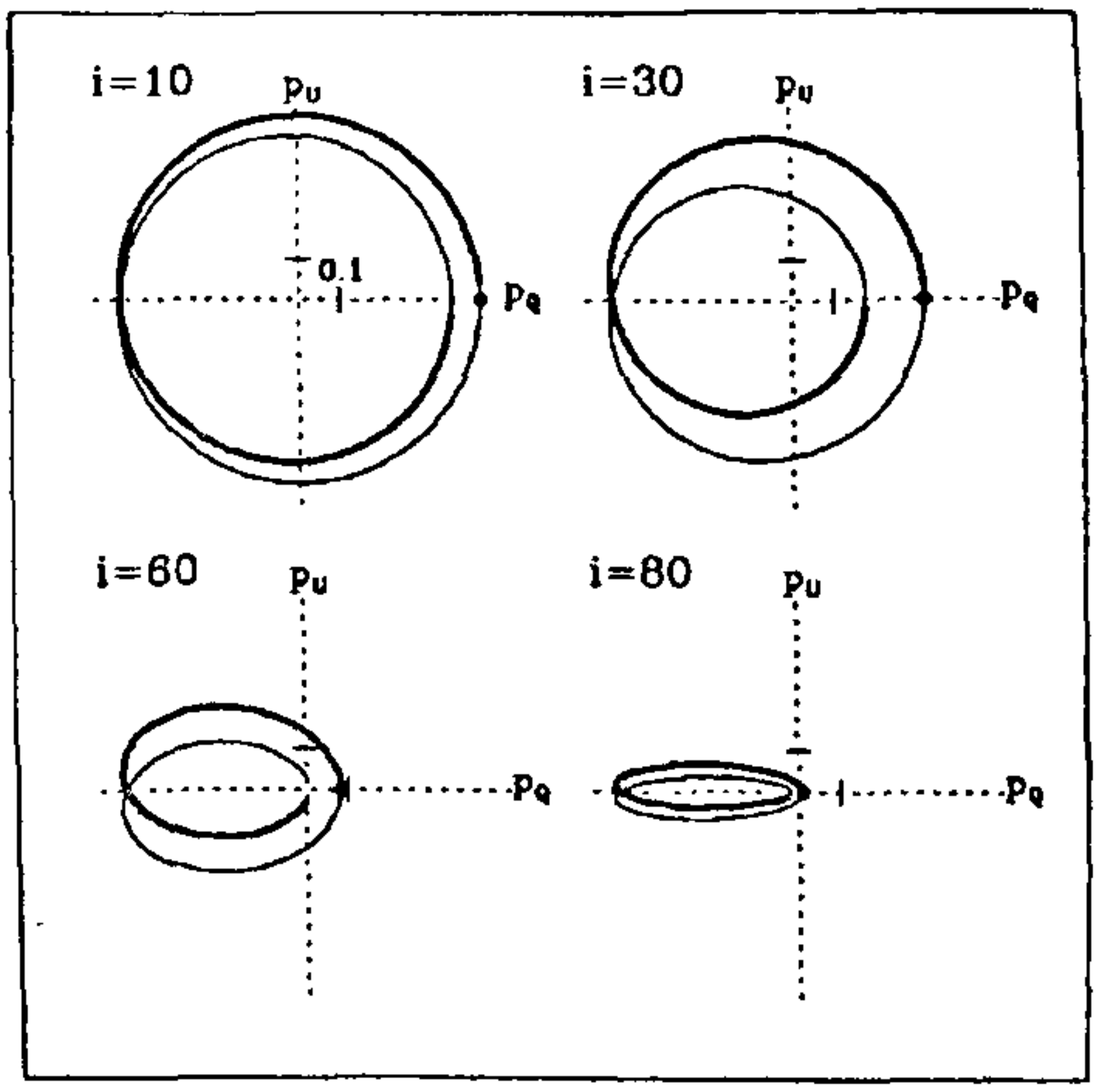

Figure 6. Expected variation of the polarization vector during one orbital period seen from different inclinations In these examples, the orientation of the ascending node is north and the rotation of the binary is anti-clockwise The phase $\omega^s 0°$ is indicated by a dot and the part of the orbit from $\omega^s 0°$ to 180° is plotted as a thick line and the rest of the orbit as a thin line.

Prospects

The polarization found in the λ6825 and λ7082 features now opens a new avenue of investigation. The geometric structure of the scatterer (H°) can be mapped in three dimensions, because the Raman scattered emission lines contain velocity and vectorial polarization information. It will be possible to map the distribution of neutral hydrogen in the outer atmosphere or wind of red giants including Mira variables. Monte Carlo simulations have already been used by Schmid to investigate the flux and polarization properties of the Raman scattered emission lines for various system configurations. The theoretical tools required to extract maximum information from such polarization measurements are being developed now.

Periodic variations of the polarization vector, due to the binary motion, will be measurable over a time span of a few years. Figure 6 shows a model calculation for the time behaviour of the polarization vector over one orbital period for a system seen at various inclinations. A time series of polarization measurements will thus permit the establishment of accurate and otherwise unobtainable orbital parameters, such as the orientation of the orbital plane relative to the observer. This technique has already been applied to other binary systems which emit polarized light like some O+O and O+WR binaries. With accurate orbital parameters for symbiotic stars, the mass ratio can be determined and it will, for example, be possible to clarify whether mass transfer to the hot companion occurs just via the stellar wind or through Roche lobe overflow and an accretion disk.

H. Schild is in the University College London, and H. M. Schmid is in the Institut für Astronomie, ETH, Zürich, Switzerland.